Hydrology and Earth System Sciences Discussions

Infiltration-soil moisture redistribution under natural conditions: experimental evidence as a guideline for realizing simulation models

R. Morbidelli, C. Corradini, C. Saltalippi, A. Flammini, and E. Rossi

Dept. of Civil and Environmental Engineering, University of Perugia, Perugia, Italy

HESSD

8, 6199–6225, 2011

Infiltration and soil moisture redistribution

R. Morbidelli et al.

Title Page

Abstract	Introduction
Conclusions	References
Tables	Figures

⏮   ⏭

◀   ▶

Back   Close

Full Screen / Esc

Printer-friendly Version

Interactive Discussion

Abstract

The evolution in time, t, of the experimental soil moisture vertical profile under natural conditions is investigated in order to address the corresponding simulation modelling. The measurements were conducted in a plot with a bare silty loam soil. The soil water content, θ, was continuously monitored at different depths, z, using a Time Domain Reflectometry (TDR) system. For each profile four buriable three-rod waveguides were inserted horizontally at different depths (5, 15, 25 and 35 cm). In addition, we used sensors of air temperature and relative humidity, wind speed, solar radiation, evaporation and rain as supports for the application of selected simulation models, as well as for the detection of elements leading to their improvement. The results indicate that, under natural conditions, very different trends of the $\theta(z,t)$ function can be observed in the given fine-textured soil, where the formation of a sealing layer over the parent soil requires an adjustment of the simulation modelling commonly used for hydrological applications. In particular, because of the considerable variations in the shape of the moisture content vertical profile as a function of time, a generalization of the existing models should incorporate a representation of the variability in time of the saturated hydraulic conductivity of the uppermost soil. This conclusion is supported by the fact that the observed shape of $\theta(z)$ can be appropriately reproduced by adopting this approach, however the observed rainfall rate and the occurrence of freeze-thaw cycles with high soil moisture contents have to be explicitly incorporated.

1 Introduction

Simulations of successive cycles of rainfall infiltration, redistribution of soil water in the no-rainfall periods and reinfiltration are needed for many hydrological applications. Usually, a simple and sufficiently accurate approach that represents on a continuous basis the evolution in time, t, of the soil moisture, θ, at different depths, z, is required. Many experiments were set up in order to show the shapes of $\theta(z,t)$ in bare soils, that were then used as guidelines for realizing the required theoretical approach.

Infiltration and soil moisture redistribution

R. Morbidelli et al.

Biswas et al. (1966) examined the function $\theta(z,t)$ within redistribution periods without evaporation by laboratory experiments for different soil types as sand, silt loam and clay loam and different cumulative infiltration depth at the beginning of the process. Similar laboratory experiments were described by Young and Poulovassilis (1976) for a sandy soil. Gardner et al. (1970a, 1970b) realized the same type of investigations on fine sandy loam soils and determined $\theta(z,t)$ during the stage of redistribution both with and without evaporation. For each of these investigations, an approximated simulation model for the reproduction of the profiles observed during redistribution was proposed (Gardner et al., 1970b).

Theoretical formulations for a continuous description of both soil moisture profiles and infiltration were proposed by several authors (see, for example, Milly (1986), Charboneau and Asgian (1991), Corradini et al. (1997, 2000)). Milly (1986) and Charboneau and Asgian (1991) include explicitly the evapotranspiration process and represent the infiltration through the classical techniques, specifically the extended Philip equation (Chow et al., 1988) combined with the "time compression approximation" (Sivapalan and Milly, 1989) and the Mein and Larson equation (Mein and Larson, 1973), respectively. Corradini et al. (1997, 2000), in principle, provide a more appropriate representation of both $\theta(z,t)$ and infiltration rate through the development of composite θ profiles, even though evapotranspiration is neglected and the formulations were tested in the limits of hydrological applications involving redistribution periods up to 20 h. In any case this duration is typically acceptable when floods due to frontal rainfalls have to be considered.

An overall analysis of our discussion indicates that sufficiently simple models of $\theta(z,t)$ are available, but their effectiveness was typically examined for a limited application field and mainly for laboratory experiments where vertical homogeneous soils were generally involved. Therefore, the existing models need to be validated and generalized on the basis of experimental data carried out in natural fields for long periods and considering that sealed soils can be found (Bullock, 1988; Emmerich, 2003).

Title Page

Abstract | Introduction

Conclusions | References

Tables | Figures

|◄ | ►|

◄ | ►

Back | Close

Full Screen / Esc

Printer-friendly Version

Interactive Discussion

The main objective of this paper is to address the above issues through continuous measurements of the basic quantities determining the evolution of $\theta(z,t)$ and by direct observations of the same function performed by a Time Domain Reflectometry (TDR) system. In this context, in order to quantify the possible errors generated by an inappropriate choice of the modelling, the effectiveness of a model based on the assumption of a vertically homogeneous soil (Corradini et al., 1997) with time invariant saturated hydraulic conductivity is compared to that of a model for a two-layered soil (Corradini et al., 2000) applied considering a sealed soil with the upper layer characterized by a time-varying saturated hydraulic conductivity, K_{1s}, and the underlying layer that keeps the properties of the parent soil. The quantity K_{1s} is determined by calibration within each specific study period, while the associated variability with time is investigated by examining the link with the experimental values of the hydrometeorological variables observed in a selected study plot of Central Italy. On this basis the main lines to follow for a further development of the pre-existing models are also given.

2 Study problem

2.1 A short description of the Corradini et al. (1997, 2000) models extended for evapotranspiration

The soil moisture vertical profile evolves under natural conditions because of the processes of rainfall infiltration and redistribution of soil water with evapotranspiration. These processes interact in determining the profile that can be investigated, as a first approximation, using one of the models earlier proposed for vertically homogeneous or layered soils. We have selected the models developed by Corradini et al. (1997, 2000) adapted by the additional effect of evapotranspiration.

The model by Corradini et al. (2000) considers the one-dimensional water flow into any two-layered soil profile under complex rainfall patterns, which produce successive infiltration-redistribution cycles. The problem formulation is simplified by assuming

the initial condition for capillary head, ψ, invariant with depth and approximating in each layer the dynamic wetting profile at a given time by a distorted rectangle represented through a shape factor β (≤ 1) which depends on the water content at the top of the layer. In each layer the model combines the continuity equation with the depth-integrated form of the Darcy law and uses the appropriate boundary conditions associated to periods with unsaturated/saturated surface together with the boundary conditions at the interface involving continuity of capillary head and water flux. Since the time when the wetting front reaches the interface, t_c, the following system of two ordinary differential equations is obtained:

$$\frac{d\psi_{10}}{dt} = \frac{1}{\alpha Z_c C_1(\psi_{10})} \left[q_{10} - E - K_{1c} - \frac{K_{1s}G_1(\psi_c, \psi_{10})}{Z_c} \right] - \frac{(1-\alpha)C_1(\psi_c)}{\alpha C_1(\psi_{10})} \frac{d\psi_c}{dt}. \quad \text{for } t \geq t_c \quad (1)$$

$$\frac{d\psi_c}{dt} = \frac{1}{P_L(\psi_c,t)}$$
$$\left[K_{1c} + \frac{K_{1s}G_1(\psi_c, \psi_{10})}{Z_c} - K_{2c} - \frac{\beta_2(\theta_{2c})p_2(\theta_{2c} - \theta_{2i})K_{2s}G_2(\psi_i, \psi_c)}{I_2} \right] \quad \text{for } t \geq t_c \quad (2)$$

with $P_L(\psi_c,t)$ defined as:

$$P_L(\psi_c,t) = \left[\beta_2(\theta_{2c}) + \frac{d\beta_2}{d\theta_{2c}}(\theta_{2c} - \theta_{2i}) \right] \frac{I_2}{(\theta_{2c} - \theta_{2i})\beta_2(\theta_{2c})} C_2(\psi_c) \quad (3)$$

I_2 being expressed through the difference:

$$I_2 = I - Z_c \left[\alpha(\theta_{10} - \theta_{1i}) + (1-\alpha)(\theta_{1c} - \theta_{1i}) \right] - K_{2i}t \quad (4)$$

where we use subscripts 1 for variables in the upper layer, 2 in the underlying soil, c at the interface, 0 at the surface, i for initial conditions, and s for the saturated conditions; Z_c is the upper layer thickness; $C(\psi) = d\theta/d\psi$; q water flux; K hydraulic conductivity; G net capillary drive; I the cumulative infiltration depth; the second term on the right hand side of Eq. (4) the cumulative dynamic infiltration depth in the upper layer; β, p

and α quantities depending on the wetting profile shape, with β explicit function of θ (Corradini et al., 1997).

Furthermore, for $t < t_c$ the wetting front moves through the homogeneous upper layer where the use of a procedure similar to that above mentioned for deriving Eqs. (1) and (2) leads to (Corradini et al., 1997):

$$C_1(\psi_{10})\frac{d\psi_{10}}{dt} = \frac{\left(q_{10} - E - K_{10} - \frac{p_1 G_1(\psi_i, \psi_{10})K_{1s}(\theta_{10} - \theta_{1i})\beta_1(\theta_{10})}{I_1}\right)}{I_1\left[\frac{1}{\beta_1(\theta_{10})}\frac{d\beta_1}{d\theta_{10}} + \frac{1}{(\theta_{10} - \theta_{1i})}\right]} \tag{5}$$

with $I_1 = I - K_{1i}t$.

The quantity E in Eqs. (1) and (5) is the evapotranspiration given by (Ragab, 1995):

$$E = E_p \cdot \text{SMI} \tag{6}$$

where SMI is the soil moisture index expressed by:

$$\text{SMI} = \begin{cases} 1 & \theta_{10} > \theta_{fc} \\ \frac{(\theta_{10} - \theta_{wp})}{(\theta_{fc} - \theta_{wp})} & \theta_{wp} \leq \theta_{10} \leq \theta_{fc} \\ 0 & \theta_{10} < \theta_{wp} \end{cases} \tag{7}$$

with θ_{fc} the field capacity defined as the bulk water content in soil at -0.33 bar pressure head and θ_{wp} the wilting point defined as the bulk water content at -15 bar pressure head; E_p is the potential evapotranspiration, given by (Maidment, 1993):

$$E_p = k_a E_v \tag{8}$$

or, alternatively, by the Penman-Monteith equation:

$$E_p = \frac{1}{\upsilon}\left[\frac{\Delta(R_n - F) + \rho c_p(e_s - e)/r_a}{\Delta + \gamma\left(1 + r_{st}/r_a\right)}\right] \tag{9}$$

with k_a empirical pan coefficient; E_v pan evaporation; υ latent heat of vaporization of water; Δ gradient of e_s as a function of temperature; R_n net incoming radiation flux; F soil outgoing heat flux; ρ and c_p density and specific heat at constant pressure of air, respectively; e_s and e saturation and actual vapour pressure, respectively; r_a and r_{st} aerodynamic and stomatal resistance, respectively; γ psychrometric constant.

By adopting for $\theta(\psi)$ and $K(\psi)$ the general functional forms used, for example, by Smith et al. (1993) and Smith (2002), numerical solutions of Eqs. (1)–(2), for sealed soils, or Eq. (5), for homogeneous soils, provide $\psi_0(t)$ and $\psi_c(t)$ or $\psi_0(t)$, respectively. In addition, through the upper boundary conditions the cumulative dynamic infiltration depth as a function of time can be determined.

The vertical profile $\theta(z)$ at each time is represented by using the function $\theta(\psi)$ to derive the values of soil moisture at specific depths. The shape of each profile is determined by the following general expression applied for homogeneous soils as well as for sealed soils:

$$\frac{\theta_x(z) - \theta_{xi}}{\theta_{xy} - \theta_{xi}} = 1 - \exp\left(\frac{\beta_x z \left(\theta_{xy} - \theta_{xi}\right) - I_x}{\left(\beta_x - \beta_x^2\right) I_x}\right) \tag{10}$$

where the subscripts x and y stand for 1 and 0, respectively, or, when the subsoil is considered, for 2 and c, respectively. Equation (10) is an extended form of that utilized by Corradini et al. (1997) for homogeneous soils. More specifically, for sealed soils, Eq. (10) is applied to the upper layer with $x = 1$, $y = 0$ and with β_1 assessed through the position $\theta_1(z = Z_c) = \theta_{1c}$ and to the lower layer with $x = 2$ and $y = c$.

An example of the results generated by Eqs. (1)–(2) and (5) is given in Fig. 1(a)–(c) where, under a steady rainfall rate followed by a redistribution period, the time-varying infiltration rate and the corresponding soil moisture profiles at a few specific times are shown for both homogeneous and sealed soils.

2.2 Experimental system

We selected a natural plot characterized by slight slope with a silty loam soil (see Table 1). The application of the explanatory models described in Sect. 2.1 requires measurements of a few classical hydro-meteorological quantities to be used specifically
5 for the simulation of the actual soil moisture profiles.

Sensors of air temperature, wind speed and direction, relative humidity and solar radiation, all operative at height of 2 m, provided the basic data for the estimate of E_p by Eq. (9); in addition a Class A evaporation pan was used for E_v of Eq. (8). A raingauge was set up in order to observe the rainfall rate that is equal to q_{10} of Eqs. (1)
10 and (5) during periods with unsaturated soil surface. In addition a TDR system was installed for the direct measurements of $\theta(z,t)$.

The water content at specific depths was monitored using the TRASE-BE device designed by the Soil Moisture Equipment Corp., Goleta, CA. Four buriable three-rod waveguides with length 20 cm were inserted horizontally at different depths along the
15 same vertical, taking care that the metal rods were in tight contact with the soil. Specifically, the probes were installed at 5, 15, 25, 35 cm depth. Each probe provided at each time a measurement of θ at the corresponding depth, but in any case the zone of influence is a small soil volume around the same probe. The reliability of the system is supported by Zegelin et al. (1989). They showed that three-wire probes imbedded
20 horizontally in a field profile during a rainfall event can be used to follow the wetting front during both infiltration and redistribution; in addition, these probes can be used to estimate the amount of infiltrated water with error less than 10 %. The four probes were interrogated at intervals of 30 min and the universal calibration curve of Topp et al. (1980) (relationship between volumetric water content and apparent dielectric
25 constant) was used to calculate θ from the TDR signal.

3   Experimental results and their analysis

Considering that small simulation errors associated to short periods could increase with time and mask the mechanisms to be clarified in this study and that the models selected were not tested for very long periods, we have chosen to investigate periods of limited duration. Therefore, many isolated events involving an infiltration period with successive redistribution/evapotranspiration of soil moisture have been investigated. Each event started from a condition of initial soil moisture that could be approximated as invariant with depth, at least in the soil part where the experimental data were available (between the probes installed at 5 and 35 cm depth). In the hypothesis of vertically homogeneous soil with constant ψ_i the shape of the curve $\theta_i(z)$ in the top soil, that is between the soil surface and 5 cm depth, has been represented by the same value of θ_i used at larger depths, while under the condition of sealed soil by the constant value giving continuity of ψ_i at the interface.

The basic quantity to be assessed in order to perform the conceptual simulations for a sealed vertical profile is the depth of the crusted layer, Z_c, that along the lines discussed by Mualem and Assouline (1989) and Mualem et al. (1993) has been set equal to 5 cm.

The application of the models described in Sect. 2.1 requires to estimate the quantities β, p and α, linked with the shape of the wetting profiles (see Corradini et al. (1997)), and those involved in the functional forms $\theta(\psi)$ and $K(\psi)$, as the Brooks-Corey pore size distribution index, λ, the air entry head, ψ_b, the empirical coefficients c and d, the saturated and residual soil water content. The last two values were associated with the maximum (0.34) and the minimum (0.092) values of θ obtained during the entire period of observation. On this basis and considering the soil structure, following Corradini et al. (1997, 2000) the remaining quantities were assessed (see Table 1). All the above quantities were assumed to be invariant from homogeneous to sealed soils. This implies that the continuity of ψ_i leads to a constant value of θ_i through the entire soil profile.

Many events in the period April 2010–December 2010 have been investigated (see Fig. 2). For each specific event the observed profiles of θ have been compared with those simulated by both the homogeneous and the two-layered model. The same value of saturated hydraulic conductivity was used in the computations for the homogeneous soil and the subsoil of the sealed profile. In particular, this value was assumed time invariant and equal to that derived by calibration events occurred in the period October 2009–March 2010, all associated with conditions of vertically homogeneous soil. Furthermore, the value of K_{1s} in the two-layered soil profile was estimated by calibration in each specific event.

The results obtained for a few events representative of the evolution in time of the processes of infiltration, redistribution/evapotranspiration during a whole year are shown in Figs. 3–9 (see also Fig. 2 and Table 2). As it can be seen in Fig. 3 the curves estimated by the model for vertically homogeneous soil, with $K_{1s} = 2\,\mathrm{mmh}^{-1}$, match appropriately with the observed values of $\theta(z)$ at the end of the rainfall as well as during the redistribution/evapotranspiration period, even though in the initial infiltration stage the agreement between theoretical simulations and experimental results does not appear fairly good probably because of inaccuracies in the TDR measurements (see also Melone et al. (2006) and Melone et al. (2008)). In addition, we found that the application of the two-layered model to the same event provided representations of $\theta(z,t)$ inconsistent with the observations. On the other hand, Figs. 4–6 show that the profiles simulated by the two-layered model, with the value of the saturated hydraulic conductivity in the topsoil obtained in each event by calibration and in the parent subsoil assessed in advance ($K_{2s} = 2\,\mathrm{mmh}^{-1}$), fit fairly well the experimental data, even though in the limit of the lack of measurements at a depth less than 5 cm. These figures indicate also that the curves computed by the homogeneous model using $K_{1s} = 2\,\mathrm{mmh}^{-1}$ have inadequate shapes, associated with substantial overestimates of the wetting front depth and cumulative dynamic infiltration. Furthermore, simulations carried out by the homogeneous model but with K_{1s} assessed by direct calibration were found in any case to provide results conflicting with the observed data.

An event occurred in the late autumn period is investigated in Fig. 7 that displays as the observed moisture contents are well simulated by the model for homogeneous soil with $K_{1s} = 2\,\mathrm{mm\,h^{-1}}$, while the existence of a crust layer, as in the event of Fig. 3, can be excluded because of the incorrect shape of the curves obtained by the sealed soil
5   model.

Two additional events, that contribute to improve the knowledge of the mechanisms determining the time-varying vertical soil structure, are examined in Figs. 8 and 9. In spite of the results are difficult to quantify because the two events start from high soil water contents, in any case they clearly suggest a similitude with Figs. 4 and 7 in
10 relation to the existence of a sealed soil and a homogeneous soil, respectively.

An overall analysis of our results indicates that during the high intensity summer thunderstorms there is a crust layer with a disturbed thickness of a few centimetres (see also Mualem and Assouline (1989) and Mualem et al. (1993)), that keeps within no rainfall periods and is associated with high soil temperature. It becomes gradu-
15 ally less permeable because of successive heavy storms, until it experiences a disruption. For example, in spite of the rainfall rate associated with Fig. 6 is halved in relation to that of Fig. 4 (see Fig. 2), the ratio K_{2s}/K_{1s} has more than doubled. Furthermore, in the late autumn the disruption of the crust layer with re-formation of a vertically homogeneous soil occurs. Then, during the successive months the infiltration-
20 redistribution/evapotranspiration events can be associated to conditions of both sealed soil and homogeneous soil.

These results can be explained in the light of the coupling, proposed by Bullock et al. (1988) through laboratory experiments, between the disruption of the crust layer and occurrence of freeze-thaw cycles under the condition of high soil water content. In
25 fact, as it can be seen in Fig. 10, the event of 24 December 2010 (Fig. 9) was preceded by many cycles of this type with air temperature, at 2 m above the ground, that dropped a few degrees below 0 °C while the soil water content at the 5 cm depth assumed values very close to soil saturation. A similar analysis can be performed for the event of 16 November 2010 (Fig. 7) when the duration of the antecedent freeze-thaw cycle

Infiltration and soil moisture redistribution

R. Morbidelli et al.

Title Page

Abstract	Introduction
Conclusions	References
Tables	Figures

◀◀   ▶▶

◀   ▶

Back   Close

Full Screen / Esc

Printer-friendly Version

Interactive Discussion

Full Screen / Esc

Printer-friendly Version

Interactive Discussion

was of about three days. This was a period more extended than that involving air temperature below 0 ˚C, because the air temperature at 2 m provides a considerable overestimate of the soil surface temperature in the nights with low wind intensity and absence of clouds. These meteorological conditions were really observed in the period aforementioned. Furthermore, in the event of Fig. 8 there was a crust with permeability larger than that of Fig. 4 because of the lower rainfall intensity involved. Lastly, from the analysis of our representative events it can be deduced that the re-formation of a crust layer can occur in any month, in the absence of freeze-thaw cycles, provided the rainfall rate is larger than a moderate threshold value.

In principle, the above results are not conflicting with the seasonal variability of the saturated hydraulic conductivity measured by Emmerich (2003) in a study area with very different climatic conditions.

4 Conclusions

Through the use of the conceptual models developed by Corradini et al. (1997, 2000), that were tested for "isolated" events by using the Richards equation as a benchmark, reliable simulations of the main characteristics of the natural soil moisture vertical profiles in bare soils are presented here. Really, this modelling has been adapted by incorporating the process of evapotranspiration, that in the "isolated" events examined here has a minor role but becomes significant when continuous applications for practical use have to be performed.

Our results indicate that, under summer thunderstorms and even for moderate rainfall rates occurring in other periods, a vertically homogeneous soil can change into a two-layered soil with a crust in the upper part. The latter keeps within no rainfall periods and becomes gradually less permeable because of successive storms of considerable intensity. The disruption of the sealing layer appears to occur through freeze-thaw cycles when high soil water contents are involved. This process was earlier suggested by Bullock et al. (1988) on the basis of laboratory experiments. Our results can be

only partly compared with those provided by Emmerich (2003), obtained through direct measurements of saturated hydraulic conductivity, because of the different distribution in time of the experiments analysed. In any case, in the limits specified, the results of the two investigations are not conflicting.

The methodologies used in the development of this work and the results we have obtained suggest that: (a) the simulation of the evolution in time of the moisture content vertical profile under natural conditions, to be used in surface and sub-surface hydrological applications concerning, for example, the formation of the overland flow and the study of the atmospheric processes requiring the water content at the soil surface as boundary condition, should rely on a sealed soil approach for the vertical profile; (b) a representation of the variability in time of the sealing layer saturated hydraulic conductivity is a crucial model requirement (see also Langhans et al. (2011)); (c) the model should represent appropriately the function $\theta(z,t)$ in a homogeneous soil when the hydraulic characteristics of the two layers are identical. The modeling adopted here verifies the points (a) and (c) but should be completed by incorporating point (b).

References

Biswas, T. D., Nielsen, D. R., and Biggar, J. W.: Redistribution of soil water after infiltration, Water Resour. Res., 2(3), 513–524, 1966.

Bullock, M. S., Kemper, W. D., and Nelson, S. D.: Soil cohesion as affected by freezing, water content, time and tillage, Soil Sci. Soc. Am. J., 52, 770–776, 1988.

Charbeneau, R. J. and Asgian, R. G.: Simulation of the transient soil water content profile for a homogeneous bare soil, Water Resour. Res., 27(6), 1271–1279, 1991.

Chow, V. T., Maidment, D. R., and Mays, L. W.: Applied Hydrology, New York, McGraw-Hill, 1988.

Corradini, C., Melone, F., and Smith, R. E.: A unified model for infiltration and redistribution during complex rainfall patterns, J. Hydrol., 192, 104–124, 1997.

Printer-friendly Version

Interactive Discussion

Corradini, C., Melone, F., and Smith, R. E.: Modeling local infiltration for a two-layered soil under complex rainfall patterns, J. Hydrol., 237, 58–73, 2000.

Emmerich, W. E.: Season and erosion pavement influence on saturated soil hydraulic conductivity, Soil Sci., 168(9), 637–645, 2003.

Gardner, W. R., Hillel, D., and Benyamini, Y.: Post-irrigation movement of soil water, 1. Redistribution, Water Resour. Res., 6(3), 851–861, 1970a.

Gardner, W. R., Hillel, D., and Benyamini, Y.: Post-irrigation movement of soil water, 2. Simultaneous redistribution and evaporation, Water Resour. Res., 6(4), 1148–1153, 1970b.

Langhans, C., Govers, G., Diels, J., Leys, A., Clymans, W., Van en Putte, A., and Valckx, J.: Experimental rainfall-runoff data: reconsidering the concept of infiltration capacity, J. Hydrol., 399(3–4), 255–262, doi:10.1016/j.jhydrol.2011.01.005, 2011.

Maidment, D. R.: Handbook of Hydrology, New York, McGraw-Hill, 1993.

Mein, R. G. and Larson, C. L.: Modeling infiltration during a steady rain, Water Resour. Res., 9(2), 384–394, 1973.

Melone, F., Corradini, C., Morbidelli, R., and Saltalippi., C.: Laboratory experimental check of a conceptual model for infiltration under complex rainfall patterns, Hydrol. Process., 20, 439–452, 2006.

Melone, F., Corradini, C., Morbidelli, R., Saltalippi., C., and Flammini, A.: Comparison of theoretical and experimental soil moisture profiles under complex rainfall patterns, J. Hydrol. Eng., 13(12), 1170–1176, 2008.

Milly, P. C. D.: An event-based simulation model of moisture and energy fluxes at a bare soil surface, Water Resour. Res., 22(12), 1680–1692, 1986.

Mualem, Y. and Assouline, S.: Modeling soil seal as a non-uniform layer, Water Resour. Res., 25, 2101–2108, 1989.

Mualem, Y., Assouline, S., and Eltahan, D.: Effect of rainfall-induced soil seals on soil water regime: wetting processes, Water Resour. Res., 29(6), 1651–1659, 1993.

Ragab, R.: Towards a continuous operational system to estimate the root-zone soil moisture from intermittent remotely sensed surface moisture, J. Hydrol., 173, 1–25, 1995.

Sivapalan, M. and Milly, P. C. D.: On the relationship between the time condensation approximation and the flux-concentration relation, J. Hydrol., 105, 357–367, 1989.

Smith, R. E.: Infiltration Theory for Hydrologic Applications, Water Resources Monograph 15, American Geophysical Union, Washington, DC, 2002.

Smith, R. E., Corradini, C., and Melone, F.: Modeling infiltration for multistorm runoff events,

Infiltration and soil moisture redistribution

R. Morbidelli et al.

Title Page

Abstract	Introduction
Conclusions	References
Tables	Figures

◄◄   ►►

◄   ►

Back   Close

Full Screen / Esc

Printer-friendly Version

Interactive Discussion

Water Resour. Res., 29(1), 133–144, 1993.

Topp, G. C., Davis, J. L., and Annan, A. P.: Electromagnetic determination of soil water content: measurements in coaxial transmission lines, Water Resour. Res., 16, 574–582, 1980.

Young, E. G. and Poulovassilis, A.: The different forms of moisture profile development during

5   the redistribution of soil water after infiltration, Water Resour. Res., 12(5), 1007–1012, 1976.

Zegelin, S. J., White, I., and Jenkins, D. R.: Improved field probes for soil water content and electrical conductivity measurement using time domain reflectometry, Water Resour. Res., 25(11), 2367–2376, 1989.

Infiltration and soil moisture redistribution

R. Morbidelli et al.

Title Page

Abstract   Introduction

Conclusions   References

Tables   Figures

◄   ►

Back   Close

Full Screen / Esc

Printer-friendly Version

Interactive Discussion

Table 1. Main characteristics of the soil used for the experiments. The quantities θ_r and θ_s denote the volumetric water content residual and at saturation, respectively. For other symbols see text. All the quantities are considered invariant from the sealing layer to the parent soil.

soil components	clay (%)	silt (%)	sand (%)	USDA textural soil classification		
	28	57	15	silty loam		
soil parameters[*]	θ_r	θ_s	ψ_b (mm)	λ	d (mm)	c
	0.092	0.34	−500	0.2	50	5

[*] Involved in the characteristic equations see Smith et al. (1993).

Title Page

Abstract | Introduction

Conclusions | References

Tables | Figures

◄◄ | ►►

◄ | ►

Back | Close

Full Screen / Esc

Printer-friendly Version

Interactive Discussion

Table 2. Main characteristics of a few simulated events representative of the observation period.

event number	date	rainfall depth (mm)	rainfall duration (h)	maximum rainfall rate within 30 min (mmh^{-1})	initial soil water content (−)
1	11 Apr 2010	19.7	11	10.9	0.282
2	26 Jun 2010	23.1	1	40.6	0.234
3	30 Jul 2010	44.0	22.5	33.4	0.145
4	14 Aug 2010	19.7	7	17.3	0.138
5	16 Nov 2010	19.3	8	10.0	0.289
6	28 Nov 2010	83.2	16	16.1	0.303
7	24 Dec 2010	23.9	21	6.0	0.311
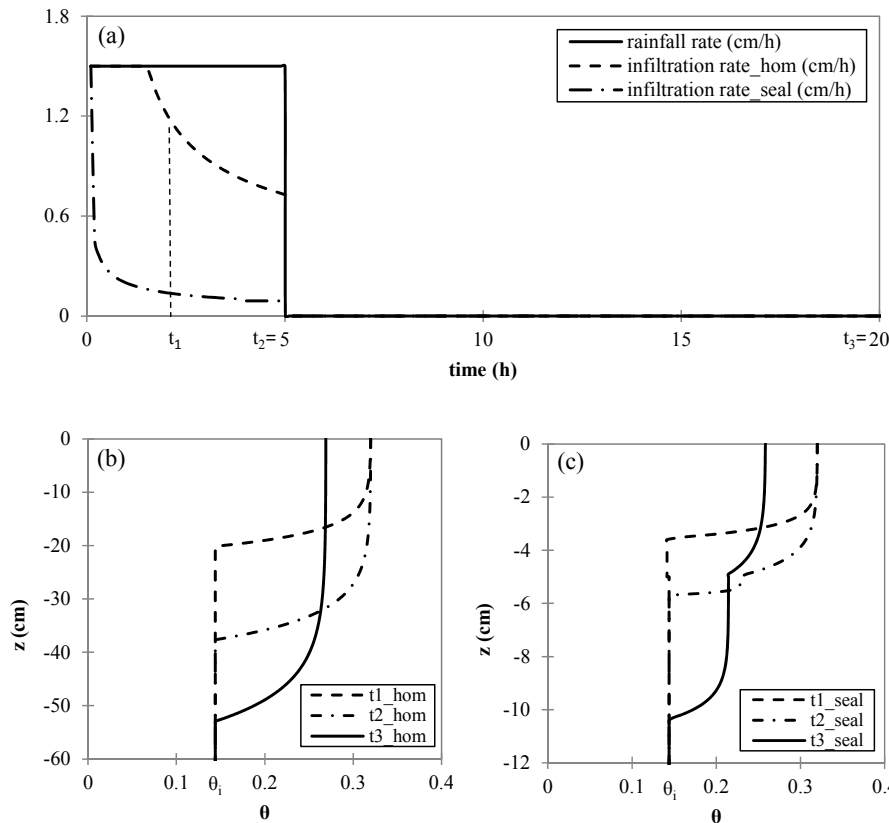
Fig. 1. (a) Time evolution of infiltration rate for homogeneous and sealed soils. **(b)** and **(c)** Vertical profiles of soil moisture at the different times indicated in the upper diagram, for homogeneous and sealed soils, respectively.
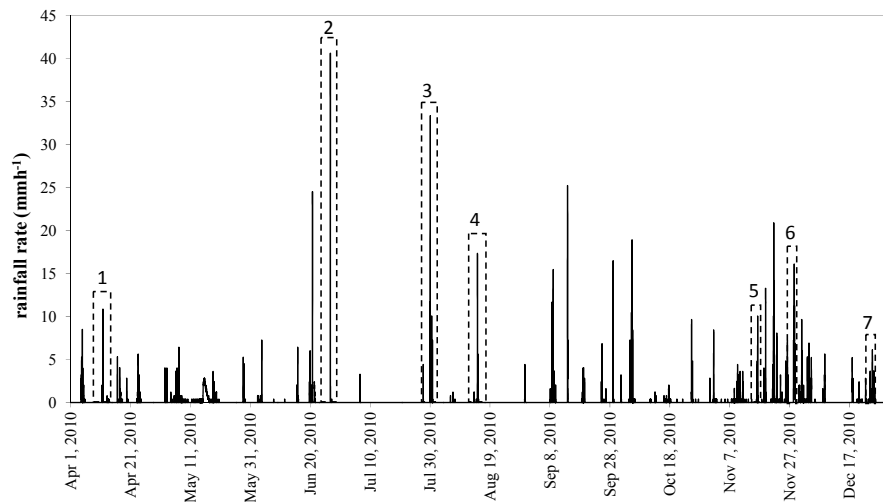
Fig. 2. Rainfall rate as a function of time observed in the study plot. The events used as representative cases in this study are indicated by the numbered dashed lines.
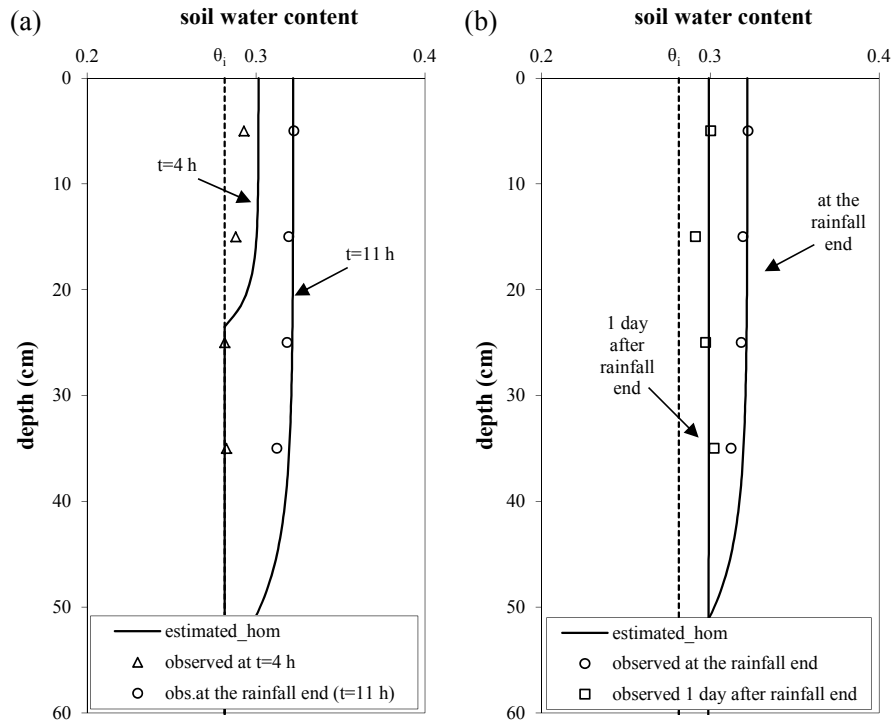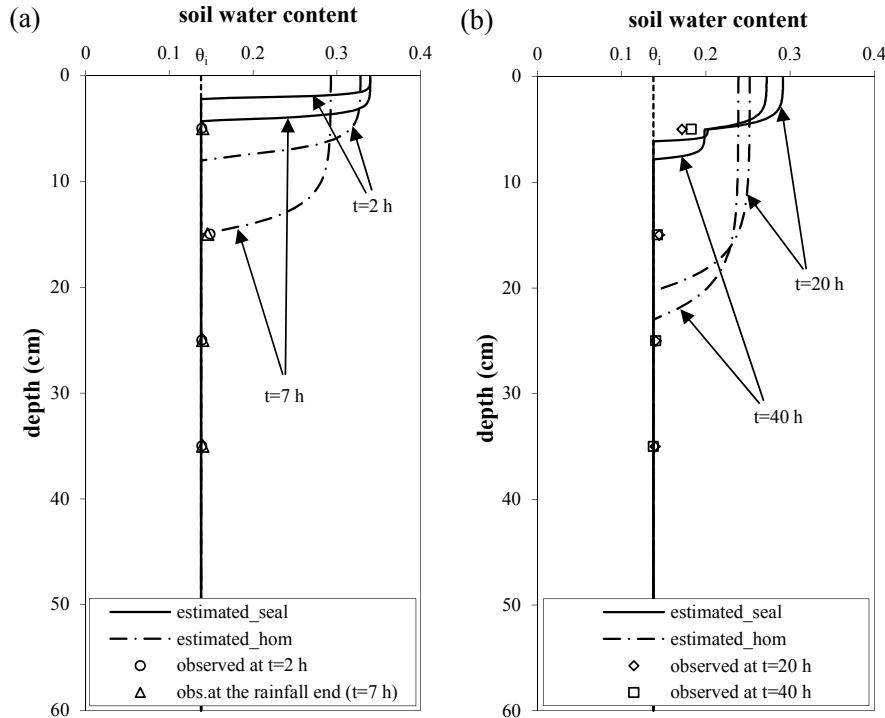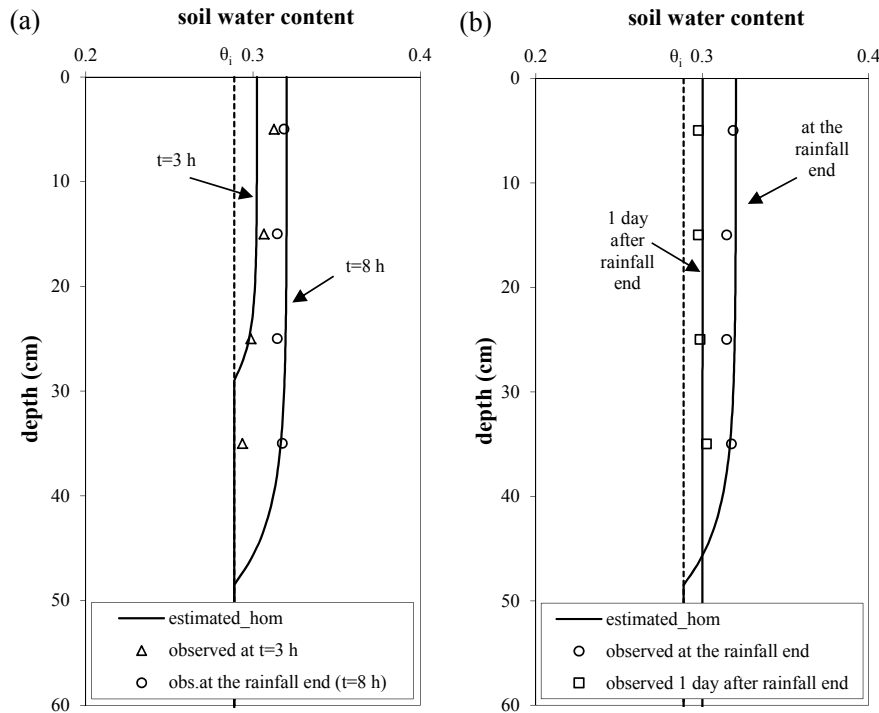
Fig. 3. Water content profiles simulated by the adopted model for homogeneous soil and specific values observed at different depths during **(a)** the infiltration stage, **(b)** the redistribution stage. Event 1 of Fig. 2 (see also Table 2). Saturated hydraulic conductivity $2\,\mathrm{mm\,h^{-1}}$.

◄◄ | ►►

◄ | ►

Back | Close

Full Screen / Esc

Printer-friendly Version

Interactive Discussion
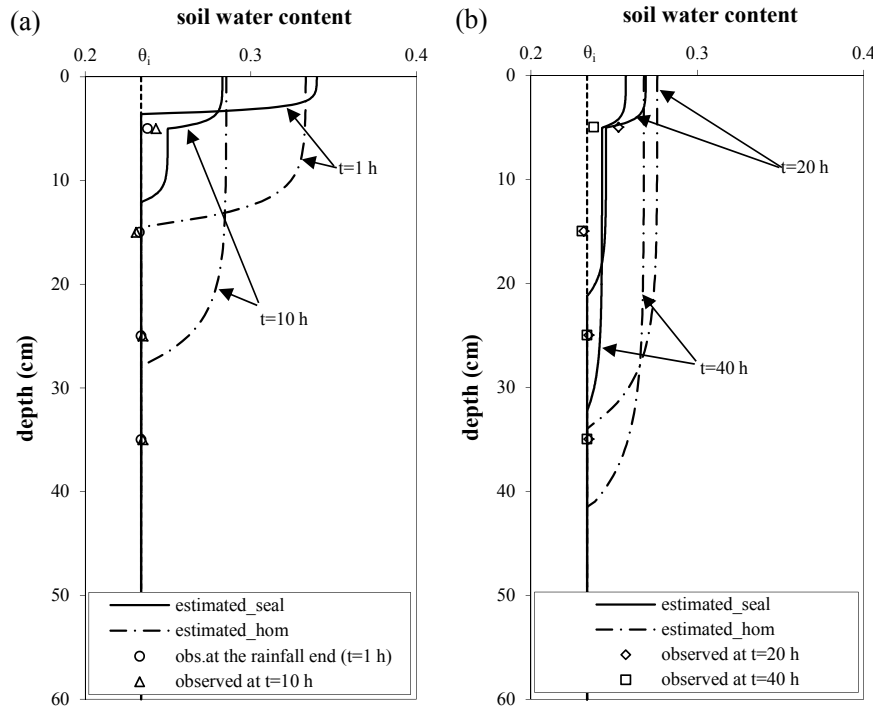
Fig. 4. Water content profiles simulated by the adopted models for homogeneous soil and sealed soil and specific values observed at different depths during different stages. Event 2 of Fig. 2 (see also Table 2). Saturated hydraulic conductivity of the parent soil $2\,\mathrm{mm\,h^{-1}}$ and seal layer $0.07\,\mathrm{mm\,h^{-1}}$.
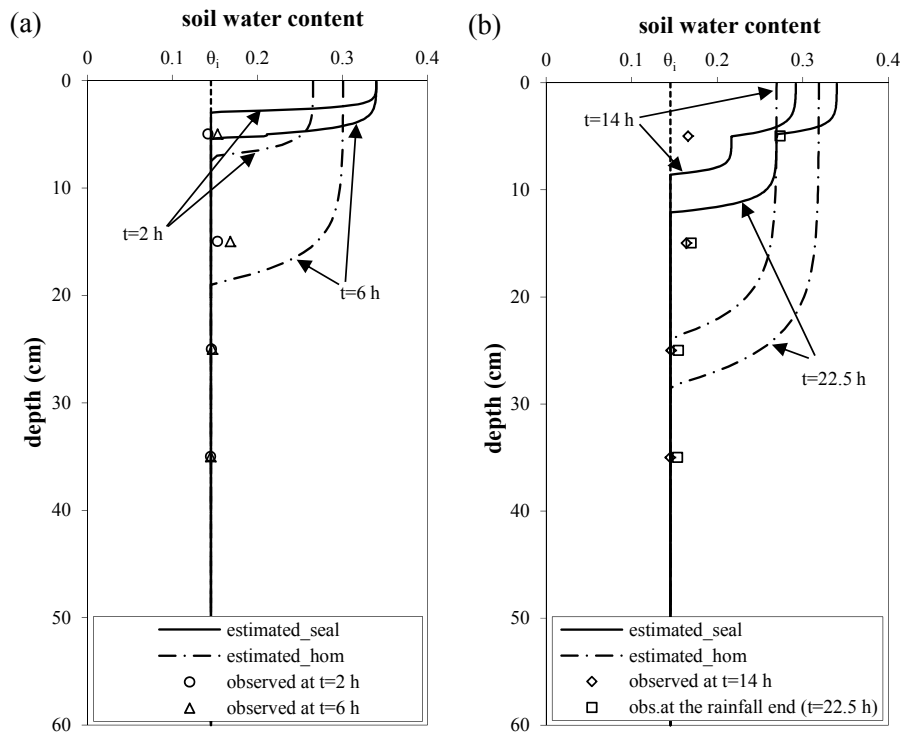
Fig. 5. Water content profiles simulated by the adopted models for homogeneous soil and sealed soil and specific values observed at different depths during different stages. Event 3 of Fig. 2 (see also Table 2). Saturated hydraulic conductivity of the parent soil 2 mmh^{-1} and seal layer 0.05 mmh^{-1}.
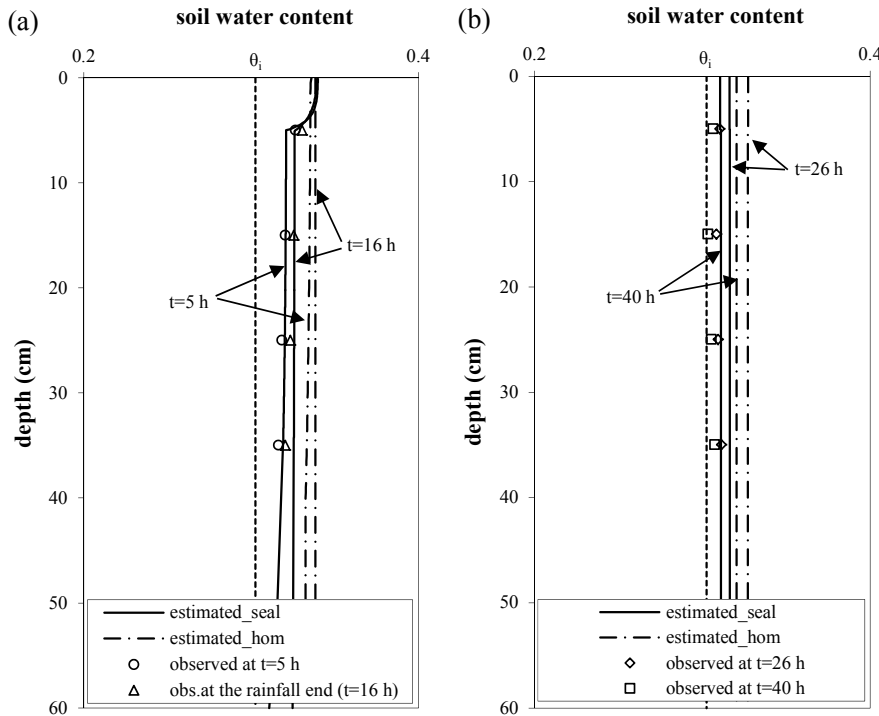
Fig. 6. Water content profiles simulated by the adopted models for homogeneous soil and sealed soil and specific values observed at different depths during **(a)** the infiltration stage, **(b)** the redistribution stage. Event 4 of Fig. 2 (see also Table 2). Saturated hydraulic conductivity of the parent soil $2\,\mathrm{mm\,h^{-1}}$ and seal layer $0.03\,\mathrm{mm\,h^{-1}}$.
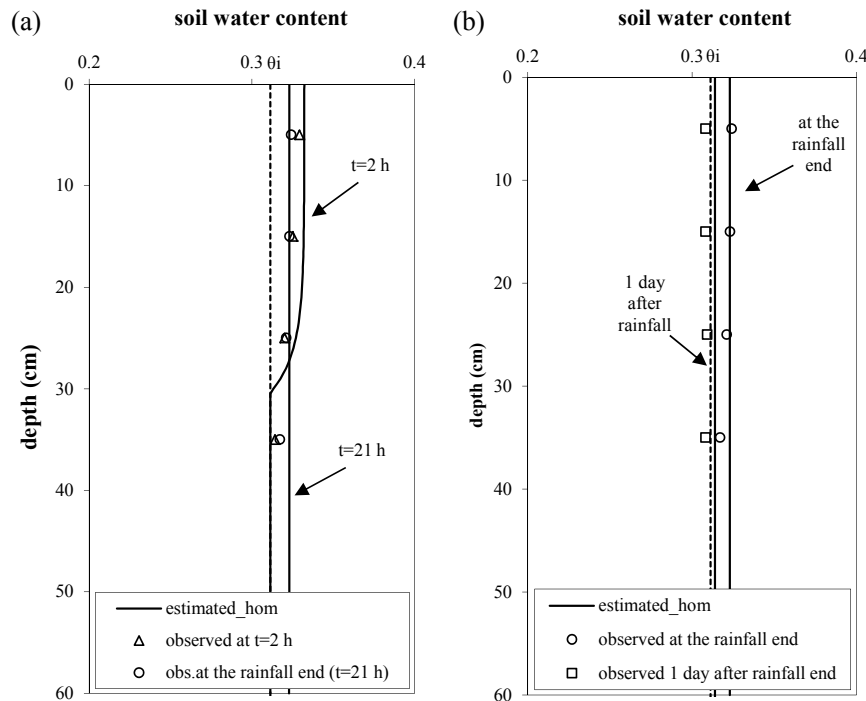
Fig. 7. Water content profiles simulated by the adopted model for homogeneous soil and specific values observed at different depths during **(a)** the infiltration stage, **(b)** the redistribution stage. Event 5 of Fig. 2 (see also Table 2). Saturated hydraulic conductivity $2\,\text{mmh}^{-1}$.

Fig. 8. Water content profiles simulated by the adopted models for homogeneous soil and sealed soil and specific values observed at different depths during **(a)** the infiltration stage, **(b)** the redistribution stage. Event 6 of Fig. 2 (see also Table 2). Saturated hydraulic conductivity of the parent soil $2\,\mathrm{mm\,h}^{-1}$ and seal layer $0.12\,\mathrm{mm\,h}^{-1}$.

Fig. 9. Water content profiles simulated by the adopted model for homogeneous soil and specific values observed at different depths during **(a)** the infiltration stage, **(b)** the redistribution stage. Event 7 of Fig. 2 (see also Table 2). Saturated hydraulic conductivity $2\,\mathrm{mm\,h^{-1}}$.
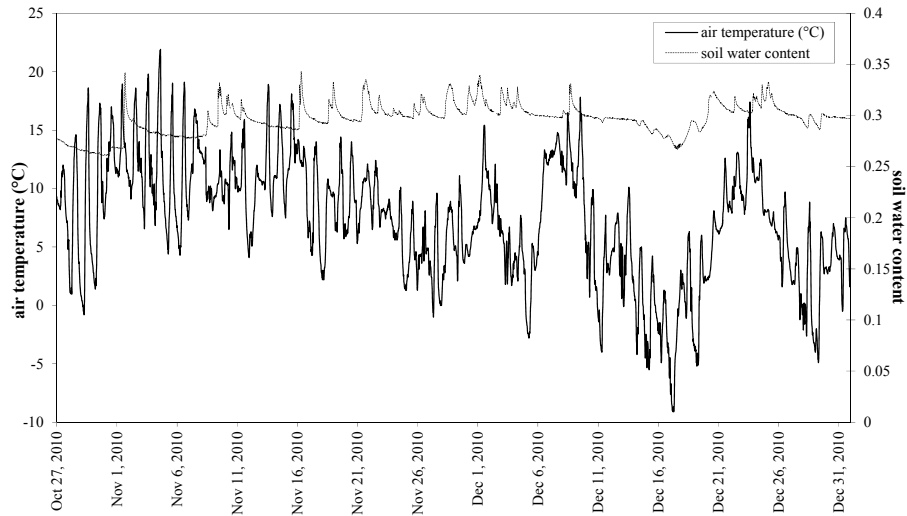
Fig. 10. Observed soil water content at 5 cm depth and air temperature at 2 m above the ground as functions of time in a limited interval of the study period.